Indonesian Physical Review

Volume 09 Issue 03, September 2026

P-ISSN: 2615-1278, E-ISSN: 2614-7904

Silver Nanoparticles as Coating for Fiber Bragg Gratings in Lead Detection

Zumrotul 'Aliyah[1], Arif Hidayat[1], Nurul Hidayat[1], Muhammad Safwan Abd Aziz[2], ST. Ulfawanti Intan Subadra[1], Ahmad Taufiq[1*]

[1]*Department of Physics, Faculty of Mathematics and Natural Sciences, Universitas Negeri Malang, Jl. Semarang 5, Malang, 65145, Indonesia*

[2]*Laser Center, Ibnu Sina Institute for Scientific and Industrial Research, Universiti Teknologi Malaysia, Skudai, Johor 81310, Malaysia*

Corresponding Author's E-mail: ahmad.taufiq.fmipa@um.ac.id

Article Info

Article info:

Received: 29-04-2026

Revised: 28-08-2026

Accepted: 10-09-2026

Keywords:

FBG; AgNPs; Lead; Silver nanoparticle

How To Cite:

Z. Aliyah, A. Hidayat, N. Hidayat, M. S. A. Aziz, ST. U. I. Subadra, A. Taufiq"Silver Nanoparticles as Coating for Fiber Bragg Gratings in Lead Detection", Indonesian Physical Review, vol. 9, no. 3, p 602-611, 2026.

DOI:

https://doi.org/10.29303/ipr.v9i3.685.

Abstract

Water pollution from heavy metals, including lead (Pb^{2+}), remains a serious problem for humanity due to their use in various industries. Although the development of water detection sensors has also been widely pursued, including etched fiber Bragg gratings (e-FBG) and tilted FBG (TFBG). FBG is unique because the optical fiber is modified, enabling it to act as a sensitive sensor for detecting Pb^{2+}. However, the existing devices require modifications that entail high costs, the need for skilled operators, and even complex preparation. Therefore, this study reports an FBG-based sensor utilizing AgNPs as a functional material for Pb^{2+} detection. Notably, the AgNPs were synthesized using laser ablation. In this study, AgNPs coating on FBGs was done to utilize localized surface plasmon resonance (LSPR), which was subsequently used for lead detection, showing a minimum detection limit of 0.65 ppm, with a sensitivity of 9.2×10^{-3} ppm/dBm, and quite selective to Pb^{2+}. Although the detection limit is not below the WHO threshold, these results demonstrate that Ag-coated conventional FBGs have potential for Pb^{2+} detection through simple, low-cost, and eco-friendly modifications. Therefore, further modifications are required to enhance the Pb detection performance of the nanoparticle coating on the FBG.

Copyright (c) 2026 by Author(s). This work is licensed under a Creative Commons Attribution-ShareAlike 4.0 International License.

Introduction

The modern world is closely tied to the use of minerals extracted from the earth for various applications [1]. Heavy metals such as lead (Pb^{2+}), arsenic (As^{3+}), cadmium (Cd^{2+}), chromium (Cr^{2+}), zinc (Zn^{2+}), and mercury (Hg^{6+}) from industrial use have been released into the water, air, and soil, causing undeniable pollution [2], [3]. To date, water pollution remains a serious problem that requires rapid and periodic detection [4], [5]. In Indonesia, many rivers have been reported to be polluted by heavy metals, especially Pb^{2+}. For example, in the Jeneberang river, the Pb^{2+} content is quite high, ranging from 30 to 50 ppm [6]. Meanwhile, the maximum threshold for Pb^{2+} in water, according to the World Health Organization (WHO), is 0.01 ppm

[7]. It has been widely used to detect water quality from heavy metals using an Atomic Absorption Spectrophotometer (AAS) [8], [9], Inductively Coupled Plasma Mass Spectrometry (ICP/MS) [10], [11], and Inductively Coupled Plasma-Atomic Emission Spectroscopy (ICP/AES) [12]. Although effective, these methods require high costs, complex preparation, and expert operators. This condition has led to the development of techniques for detecting heavy metals in water that are easier and more effective in various ways.

Optical sensors have advantages, including resistance to electromagnetic interference and high stability even when exposed to extreme temperatures, pressure, and humidity [13]. One of the efforts to develop heavy metal detection is to utilize fiber bragg gratings (FBG), which specifically use evanescent waves in surface plasmon resonance [14], [15]. Although FBG-based sensors are often used to measure load, strain, voltage, and temperature, coating certain nanomaterials as external modifications can also improve their efficiency in heavy metal detection [16], [17]. In addition, some attempts to make it into a heavy metal sensor, in addition to coating nanomaterials directly, are by etching FBG (e-FBG) and tilted FBG (TFBG) [18], [19]. These efforts have demonstrated that fiber optics can detect heavy metals. Previous research showed that the use of e-FBG is able to detect Pb^{2+} with a low detection limit of up to 10 fM [20].

Both eFBGs and TFBGs exhibit enhanced sensitivity to interactions between the optical field and the surrounding environment, driven by changes in the surface refractive index. These changes are achieved by modifying the fiber structure, such as by reducing the cladding in eFBGs or by using tilted gratings in TFBGs. In eFBGs, the etching process using strong hydrofluoric acid renders the fibers brittle and prone to damage, whereas TFBGs involve more complex data interpretation due to their sensitivity to bending direction. Furthermore, both types require specialized structural modifications, resulting in higher costs [21], [22]. In contrast, this study employs conventional FBGs and evaluates the extent to which nanocomposites can serve as active materials without structural modifications. Furthermore, conventional FBGs are less expensive than structurally modified FBGs, which are quite costly despite still requiring coating modifications. Even so, the study still needs further development to detect heavy metals.

To enhance the performance of the FBG-based heavy metal detector, this study modified the FBG with nanoparticles. Nanoparticles have various advantages that can improve performance. Silver nanoparticles (AgNPs) are one of the materials that have been in demand due to their many unique properties, including their extraordinary plasmonic properties [23]. The optical properties of these nanoparticles, which exhibit specific absorption of localized surface plasmon resonance (LSPR), make them very likely to be able to detect chemical substances [24], [25]. Previous research has also proven that AgNPs sensors can detect heavy metals Pb^{2+} in water up to 13.6 μM [26],[27]. This reinforces the use of AgNPs as FBG coatings for further development of heavy metal detection. However, in that study, AgNPs were synthesized using chemicals such as silver nitrate, sodium borohydride, hydrazine hydrate, sodium citrate, and lithium aluminum hydride.

The use of these chemicals does not rule out the possibility of secondary pollutants that are harmful to the environment. Therefore, in this study AgNPs were synthesized by laser ablation, a method considered safer and more environmentally friendly than chemical methods because it requires no additional chemicals and uses only water and a laser [28]. In addition, the AgNPs-coated FBG sensor configuration features a simpler structure and is easier to fabricate than several previous studies that require optical fiber modifications, a distinct advantage of this study. Therefore, this study was conducted to demonstrate the performance of AgNPs-coated FBGs for Pb^{2+} detection in water, which offers structural simplicity, sensor stability, environmental friendliness, and potential for further development.

Experimental Method

In this experiment, an FBG with a center wavelength of 1559.887 nm is used, coated with AgNPs. The synthesis of AgNPs is carried out by laser ablation, and before firing, the bulk 99.9% silver is first rubbed with sandpaper and sonicated for 10 minutes. Laser ablation was performed with a Ytterbium laser fiber RFL 20 at a wavelength of 1064 nm with 90% power (20 watts of the maximum energy) and a speed of 1000 mm/s for 2 minutes. A cleaned piece of pure silver bulk was placed in a cuvette with 4 mL of water for laser irradiation. The parameters used, including the time, were kept constant during nanoparticle synthesis.

Subsequently, AgNPs were prepared for XRD, UV-Vis, and SEM-EDX analysis. The AgNPs solution was deposited onto a 1 × 1 cm glass slide. This is because the AgNPs, initially in liquid colloid form, need to be solidified for characterization by XRD and SEM, as these techniques cannot be performed on liquid samples. Then, the sample was characterized using XRD, UV-Vis, and SEM-EDX to determine its structure, absorbance, morphology, and elemental composition.

Before coating, FBG is cleaned with Isopropyl Alcohol and methanol. After drying, the FBG is soaked in 1 M NaOH and then cleaned with deionized water. Next, after cleaning and drying again, the FBG is soaked in Mercaptopropyl-trimethoxysilane (MPTMS) for 24 hours, then cleaned again with ethanol and soaked with AgNPs until dry. Once dry, FBG can be used to detect heavy metals using an Optical Spectrum Analyzer (OSA). Pb^{2+} samples were prepared by making 10 – 50 ppm solutions from $Pb(NO_3)_2$. The Pb^{2+} solutions were placed in the well of the container with an FBG connected to an OSA and a light source. After connection, the Pb^{2+} concentration was varied, and the sample was positioned at the Bragg location, and OSA data were then collected to determine sensitivity. Selectivity was assessed by varying the heavy metals while keeping the concentration constant.

Result and Discussion

The analysis of the diffraction pattern and structure of AgNPs is shown by the X-ray diffraction results in Figure 1. Based on Figure 1 (a), AgNPs have a crystalline diffraction pattern visible at the apex 2θ = 37.99 °, 44.15 °, 64.21 °, and 77.10 ° with hkl planes (111), (200), (220), and (311), with lattice parameters of 4.0995 Å. This pattern is in accordance with the AMCSD database No. 0011135, which also indicates that the crystal structure of AgNPs is face-centered cubic (FCC) with the space group Fm-3m ($\alpha = \beta = \gamma = 90^0$), as in Figure 1(b). This is also in line with the diffraction pattern of AgNPs observed in previous research, which reported AgNPs diffraction patterns corresponding to hkl (111), (200), (220), and (311) and a cubic crystal structure [26], [29]. These analysis results show that AgNPs were successfully synthesized without any impurities.

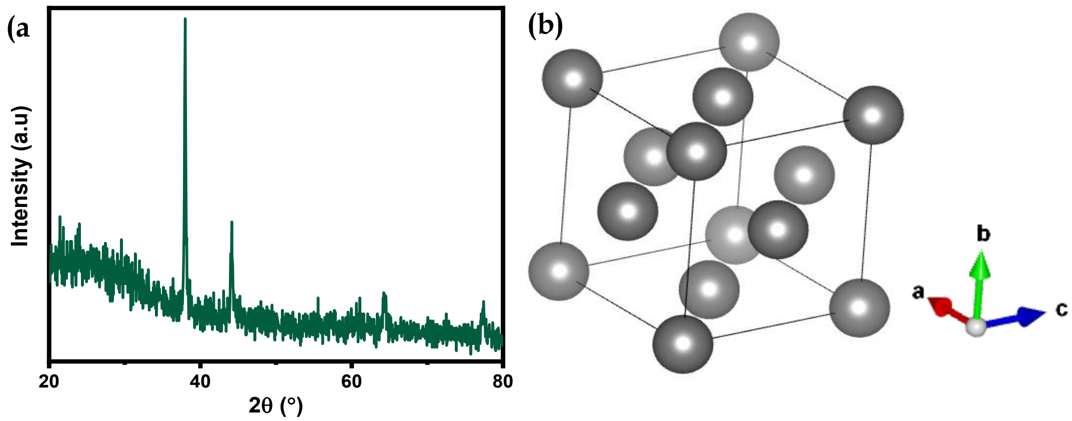

Figure 1. (a) XRD Analysis (b) Crystal Structure of AgNPs

Furthermore, the UV-Vis spectrum of AgNPs is shown in Figure 2. AgNPs appear to have a peak around 400 nm. The peak indicates the presence of LSPR, which is characteristic of AgNPs. Furthermore, this peak is close to the absorbance results previously studied, namely at a wavelength of 421 nm [30]. AgNPs are metallic materials; the absorption band originates from LSPR. These characteristics support the formation of AgNPs with the synthesis method in this study, although results from other characterizations are also needed to confirm that. Then, the high absorbance intensity indicates the significant formation of AgNPs in the colloid [31].

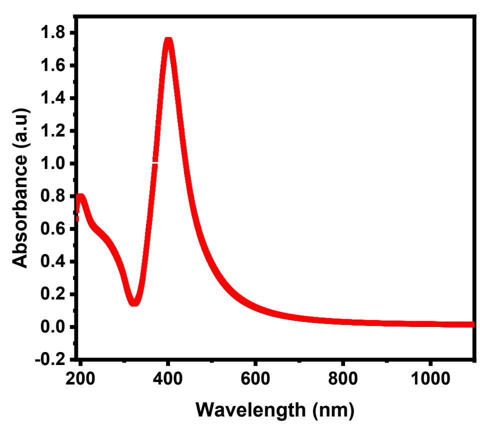

Figure 2. Analysis of UV-Vis Spectrometer

The morphology of AgNPs was analyzed using a Scanning Electron Microscope-Energy Dispersive X-ray (SEM-EDX), and the results are shown in Figure 3. These nanoparticles were synthesized in colloidal form and required drying on a glass substrate for SEM-EDX testing, which requires a solid sample. EDX analysis revealed the presence of AgM and AgL elements at around 0.5 keV and 2.8 keV, respectively, representing the AgNPs in the colloid [32]. Si, O, Mg, Ca, and Na were also found in this colloid in significant amounts due to the glass sample preparation used in the test [33].

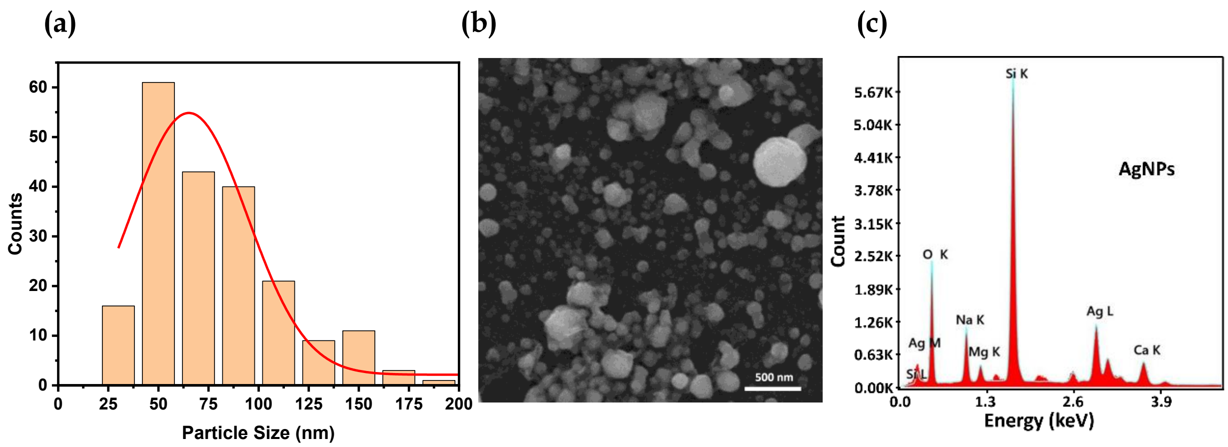

Figure 3. SEM-EDX Analysis of AgNPs.

Based on SEM analysis, the average particle size of AgNPs is 65.2 nm with a spherical shape. The average AgNPs size commonly found is 1-100 nm, and previous research has reported an average AgNPs size of 48 nm [34]. AgNPs can possess a large surface area due to their nanoscale dimensions, resulting in enhanced light absorption and effective interaction with target molecules [35]. This size can be adjusted, or made smaller or larger, by changing the ablation parameters [36]. However, SEM images indicate that each particle tends to agglomerate. In theory, colloidal nanoparticles often easily experience aggregation between particles because the ratio between the surface and volume is too large [37]. Therefore, AgNPs coating on the FBG must be performed on a new sample to avoid nanoparticle agglomeration.

In this study, the sensor's performance in detecting Pb^{2+} was evaluated using sensitivity and selectivity tests. The performance of the AgNPs-coated FBG as a Pb^{2+} heavy-metal detection sensor has been tested, with the results shown in Figure 4. Based on Figure 4 (a), it is known that the AgNPs-coated FBG is able to detect the presence of Pb^{2+} with a sensitivity of 9.2×10^{-3} dBm/ppm (Figure 4 (b)). Furthermore, the lowest detection limit of this sensor has been calculated using Equation (1), yielding 0.65 ppm within the 10–50 ppm detection range. As with previous studies, AgNPs have been proven to be able to detect Pb^{2+} with a detection limit of 37×10^{-9} M [38], [39]. Figure 4(c) is a graph of sensor selectivity, showing that the sensor exhibits a significant response to Pb^{2+} relative to Cd^{2+}, Zn^{2+}, and Cu^{2+}. These results prove that the use of AgNPs also provides quite good selectivity to Pb^{2+} compared to other heavy metals [40].

$$LoD = \frac{3.3 \times \sigma}{s} \quad (1)$$

Where σ is the standard deviation or standard error, while s is the slope of the sensor linearity [41].

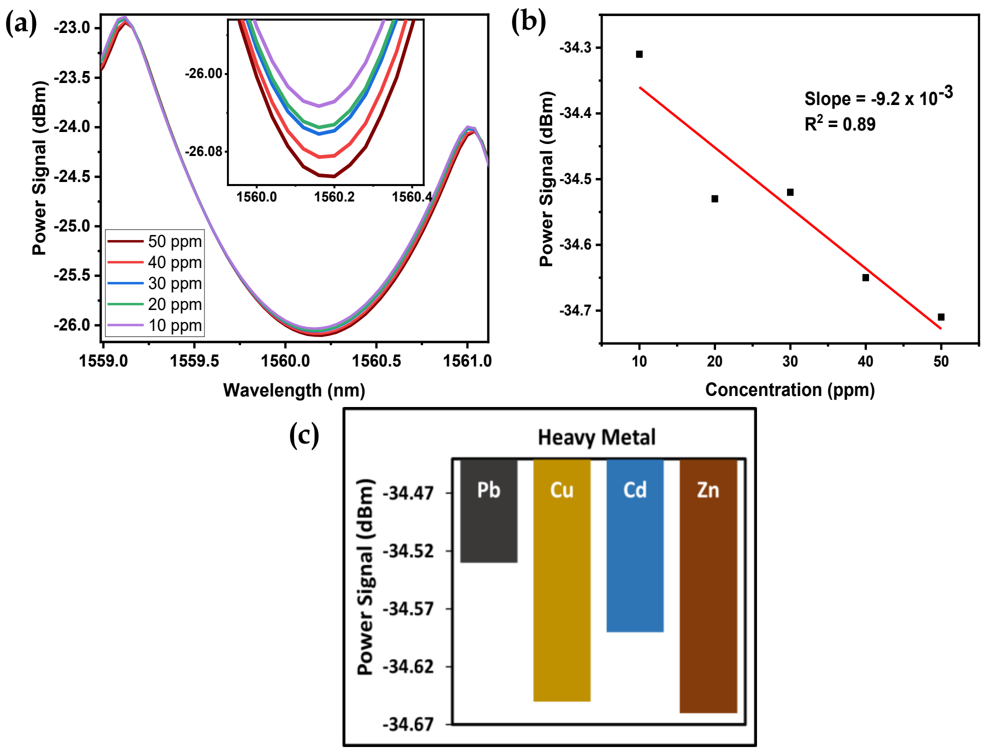

Figure 4. (a) Peak Position, (b) Sensitivity, and (c) Selectivity of Pb^{2+} Sensor.

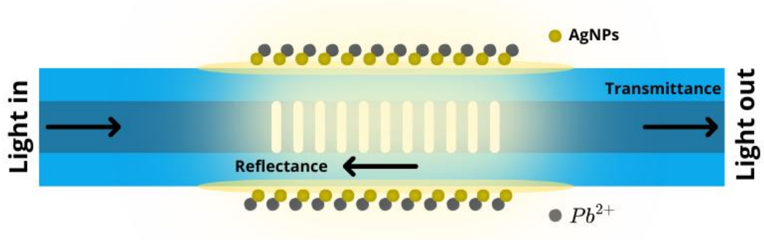

Figure 5. Pb^{2+} Sensor Detection Mechanism.

Next, the heavy metal detection mechanism using FBG-based AgNPs is shown in Figure 5. AgNPs will cooperate with Pb^{2+}, so that it changes the external conditions of the FBG and makes a change in wavelength compared to before the presence of AgNPs, as well as a change in signal strength if there is a difference in heavy metals [16], [42]. MPTMS, in this case, functions as an activator of the -OH group to bond AgNPs to the FBG [43]. By coating MPTMS first, AgNPs can adhere well to the FBG, thereby improving its performance in detecting Pb^{2+}. In the FBG concept, incoming light waves exit in two paths; some are transmitted, and others are reflected. This occurs due to the principle of Bragg reflection with periodic refractive index modulation that is capable of reflecting very well, and the other is transmitted through the grating [44]. But, this experiment shows that detecting Pb^{2+} based on signal intensity change, because the change in Pb^{2+} concentration only causes loss of the cladding mode and not enough to change the global refractive index, so the wavelength does not shift [19].

Several previous studies have also successfully applied FBGs to detect Pb^{2+} in water using various techniques such as FBG etching and TFBG. FBG etching-based sensors have demonstrated the ability to detect Pb^{2+} with a sensitivity of 5×10^{-3} nm/ppm over the concentration range of 0–50 ppm [45]. In addition, it has also been reported that Black Phosphorus coating on TFBG showed a sensitivity of 0.5×10^{-3} dB/ppb and a detection limit of 0.25 ppb, and when TFBG was coated with gold (Au) and thrombin aptamer, the detection limit was low, reaching 0.001 ppb [46], [47]. Not only that, TFBG with graphene oxide (GO) and Au coating showed a sensitivity of 0.018 dB/μM and a detection limit of 0.711 μM on Pb^{2+} [19]. This demonstrates that coating FBGs with various materials can improve sensor performance and that high sensitivity arises from structural modifications in TFBGs and eFBGs. Without structural modifications, this research will focus more on the effects of the AgNPs coating. However, this research focuses primarily on the functionality of AgNPs as an FBG coating for Pb^{2+} detection. Although the detection limit of this study does not yet meet the WHO-recommended maximum Pb^{2+} threshold of 0.01 ppm, this sensor has the potential to serve as an initial monitoring tool for detecting Pb^{2+} contamination using a simpler system.

Conclusion

FBG, which is usually a strain and temperature sensor, can also detect Pb^{2+} ions well. The use of AgNP coatings as functional materials exhibiting the LSPR phenomenon is very helpful for FBGs in detecting heavy metals. The AgNPs produced via laser ablation are spherical and 65.2 nm in size. It is also driven by the small particle size and the remarkable optical properties of AgNPs produced by laser ablation. In this case, the detection of Pb^{2+} showed sensitivity and selectivity, with a detection limit of 0.65 ppm. Although the resulting detection limit remains higher than the WHO threshold for the heavy metal Pb^{2+} in water. This study has contributed to the development of AgNPs as a functional material for FBG-based Pb^{2+} detection. Even so, improving the performance of FBG remains necessary, and it is hoped that future research will develop FBG coatings using AgNPs compositions combined with other nanomaterials.

Acknowledgment

This research was funded by the Ministry of Education and Science through the Regular Fundamental Research Scheme (PFR) with Contract No. 2.6.61/UN32.14.1/LT/2025.

References

[1] N. Soltani, B. Keshavarzi, F. Moore, A. Sorooshian, and M. R. Ahmadi, “Distribution of potentially toxic elements (PTEs) in tailings, soils, and plants around Gol-E-Gohar iron mine, a case study in Iran,” *Environ Sci Pollut Res*, vol. 24, no. 23, pp. 18798–18816, Aug. 2017.

[2] M. Moghimi Dehkordi, Z. Pournuroz Nodeh, K. Soleimani Dehkordi, H. Salamanvandi, R. Rasouli Khorjestan, and M. Ghaffarzadeh, “Soil, air, and water pollution from mining and industrial activities: Sources of pollution, environmental impacts, and prevention and control methods,” *Results in Engineering*, vol. 23, p. 102729, Sep. 2024.

[3] M. Rusdi *et al.*, “Synthesis of magnetite-CS/AC/titania nanocomposite for heavy metal (Cu) adsorption,” *AIP Conf. Proc.*, vol. 3068, no. 1, Aug. 2024.

[4] N. S. Febrianti, A. Taufiq, A. Hidayat, N. Mufti, and S. T. U. I. Subadra, “Synthesis and Characterization of ZnFe2O4- PEG/RGO Nanocomposites as Lead Heavy Metal Adsorbents,” *Key Engineering Materials*, vol. 941, pp. 155–163, 2023.

[5] M. D. Setiana, Y. W. Fen, A. Hidayat, S. U. I. Subadra, and A. Taufiq, "Synthesis of Magnetite/Activated Carbon Nanocomposites for the Removal of Lead and Methylene Blue," *Indonesian Physical Review*, vol. 9, no. 2, pp. 286–301, Apr. 2026.

[6] Aryani Ahmad, Rahman, and Hidayat, "Studi Kandungan Logam Berat Timbal (Pb) pada Sedimen dan Air di Sungai Jeneberang Kota Makassar 2020," *Window of Public Health journal*, vol. 2, no. 5, Oct. 2021.

[7] World Health Organization, Ed., *Guidelines for drinking-water quality*, Fourth edition incorporating the first addendum. Geneva: World Health Organization, 2017.

[8] N. S. A. Kassim, S. A. I. S. M. Ghazali, F. Liyana Bohari, and N. A. Z. Abidin, "Assessment of heavy metals in wastewater plant effluent and lake water by using atomic absorption spectrophotometry," *Materials Today: Proceedings*, vol. 66, pp. 3961–3964, Jan. 2022.

[9] S. K. Rai, R. Xalxo, T. K. Patle, A. Verma, R. Chauhan, and P. K. Mahish, "Analyzing Contamination of Heavy Metals - AAS and Fluorescence Spectroscopy," in *Heavy Metals in the Environment: Management Strategies for Global Pollution*, vol. 1456, in ACS Symposium Series, no. 1456, vol. 1456., American Chemical Society, 2023, pp. 167–204.

[10] Y. Li *et al.*, "Assessment of health risk and identification of pollution sources of heavy metals in water in Chongqing's wastewater treatment plants based on ICP-MS," *Environmental Pollution*, vol. 373, p. 126193, May 2025.

[11] I. A. Alhagri, A. N. Al-Hakimi, S. M. Al-Hazmy, and A. E. A. E. Albadri, "Determination of trace and heavy metals in bottled drinking water in Yemen by ICP-MS," *Results in Chemistry*, vol. 8, p. 101558, Jun. 2024.

[12] M. A. Akl, M. A. Hashem, M. A. Ismail, and D. A. Abdelgalil, "Novel diaminoguanidine functionalized cellulose: synthesis, characterization, adsorption characteristics and application for ICP-AES determination of copper (II), mercury (II), lead (II) and cadmium (II) from aqueous solutions," *BMC Chemistry*, vol. 16, no. 1, p. 65, Aug. 2022.

[13] F. Ama *et al.*, "THE APPLICATION OF PLASTIC FIBER OPTIC SENSOR AS BLOOD PRESSURE MONITORING," *Indonesian Physical Review*, vol. 8, no. 1, pp. 300–314, Jan. 2025.

[14] H. A. Mohammed, A. Almamori, and A. A. Alwahib, "Cladding Modified Fiber Bragg Grating for Copper Ions Detection," *Semicond. sci. and inf. n.a.*, vol. 3, no. 2, pp. 12–16, Nov. 2021.

[15] W. Hardianto, B. Arminah, and A. Arifin, "Detection of Mercury Ions in Water using a Plastic Optical Fiber Sensor," *Indonesian Physical Review*, vol. 4, no. 2, pp. 95–103, Jun. 2021.

[16] S. Ghosh, K. Dissanayake, S. Asokan, T. Sun, B. M. A. Rahman, and K. T. V. Grattan, "Lead (Pb2+) ion sensor development using optical fiber gratings and nanocomposite materials," *Sensors and Actuators B: Chemical*, vol. 364, p. 131818, Aug. 2022.

[17] G. A. Bodkhe *et al.*, "Enhanced detection of heavy metal ions using Ag nanoparticles and single-walled carbon nanotubes within Cu-based metal-organic frameworks," *Journal of Environmental Chemical Engineering*, vol. 12, no. 3, p. 113024, Jun. 2024.

[18] S. Mohan and N. Kumar, "Etched FBG-Based Optical Fiber Sensor for Hg^{2+} Ion Detection in Aqueous Solution," *IEEE Photonics Technology Letters*, vol. 36, no. 21, pp. 1289–1292, Nov. 2024.

[19] W. Udos *et al.*, “Surface plasmon sensor for lead ion (Pb2+) detection using graphene oxide – Gold coated tilted fiber Bragg grating,” *Results in Optics*, vol. 12, p. 100502, Jul. 2023.

[20] N. V. Kumar, B. S. Kavitha, and S. Asokan, “A Silver Nanoparticle Modified Etched Fiber Bragg Grating Sensor for Arsenic Detection,” *IEEE Sensors Journal*, vol. 23, no. 20, pp. 24518–24525, Oct. 2023.

[21] Q. Jiang, “A comparison study of the sensing characteristics of FBG and TFBG,” *Sensor Review*, vol. 33, pp. 68–79, Jan. 2013.

[22] V. Naik Parrikar *et al.*, “Sub-nanometer scale investigation of polyelectrolyte adsorption and desorption processes using etched fiber Bragg grating technique,” *Commun Chem*, vol. 8, no. 1, p. 208, Jul. 2025.

[23] A. Naganthran *et al.*, “Synthesis, Characterization and Biomedical Application of Silver Nanoparticles,” *Materials*, vol. 15, no. 2, p. 427, Jan. 2022.

[24] S. Rasheed *et al.*, “Integration of LSPR-based colorimetric sensing and smartphone-assisted dual read-out microfluidic paper-based analytical devices for rapid detection of Pb2+ in environmental samples,” *Measurement*, vol. 239, p. 115519, Jan. 2025.

[25] M. El Barghouti, A. Akjouj, and A. Mir, “Design of silver nanoparticles with graphene coating layers used for LSPR biosensor applications,” *Vacuum*, vol. 180, p. 109497, Oct. 2020.

[26] F. Sudarman, M. Shiddiq, B. Armynah, and D. Tahir, “Silver nanoparticles (AgNPs) synthesis methods as heavy-metal sensors: a review,” *Int. J. Environ. Sci. Technol.*, vol. 20, no. 8, pp. 9351–9368, Aug. 2023.

[27] R. Chanajaree, C. Ratanatawanate, S. Ruangchaithaweesuk, V. S. Lee, and K. Wittayanarakul, “Colorimetric detection of Pb2+ ions using curcumin silver nanoparticles,” *Journal of Molecular Liquids*, vol. 343, p. 117629, Dec. 2021.

[28] M. C. Sportelli *et al.*, “The Pros and Cons of the Use of Laser Ablation Synthesis for the Production of Silver Nano-Antimicrobials,” *Antibiotics (Basel)*, vol. 7, no. 3, p. 67, Jul. 2018.

[29] M. Khatamifar, S. J. Fatemi, M. Torkzadeh-Mahani, M. Mohammadi, and M. Hassanshahian, “Green and eco-friendly synthesis of silver nanoparticles by Quercus infectoria galls extract: thermal behavior, antibacterial, antioxidant and anticancer properties,” *Particulate Science and Technology*, vol. 40, no. 3, pp. 281–289, Apr. 2022.

[30] I. Urio and A. Mahadhy, “Silver nanoparticle-enhanced UV–Vis assay for rapid detection of Escherichia coli in milk,” *Appl Nanosci*, vol. 15, no. 5, p. 39, Sep. 2025, doi: 10.1007/s13204-025-03117-7.

[31] P. Lodeiro, E. P. Achterberg, and M. S. El-Shahawi, “Detection of silver nanoparticles in seawater at ppb levels using UV–visible spectrophotometry with long path cells,” *Talanta*, vol. 164, pp. 257–260, Mar. 2017.

[32] B. M. Dayana *et al.*, “Biosynthesis of silver nanoparticles via Melaleuca alternifolia leaf extract for antibacterial, antifungal, antioxidant and anticancer activity,” *Sci Rep*, vol. 16, no. 1, p. 2574, Jan. 2026.

[33] Most. N. YeasmiN, M. Sultana, A. SïDdïKa, S. Tabassum, S. Mahmud Ullah, and M. S. Bashar, “Structural, Optical, and Morphological Characterization of Silica Nanoparticles Prepared by Sol-Gel Process,” *Journal of the Turkish Chemical Society Section A: Chemistry*, vol. 9, no. 4, pp. 1323–1334, Nov. 2022.

[34] D. Jaskulski, I. Jaskulska, J. Majewska, M. Radziemska, A. Bilgin, and M. Brtnicky, "Silver Nanoparticles (AgNPs) in Urea Solution in Laboratory Tests and Field Experiments with Crops and Vegetables," *Materials*, vol. 15, no. 3, p. 870, Jan. 2022.

[35] A. Almatroudi, "Silver nanoparticles: synthesis, characterization and biomedical applications," *Open Life Sci*, vol. 15, no. 1, pp. 819–839, Nov. 2020.

[36] A. Balachandran, S. P. Sreenilayam, K. Madanan, S. Thomas, and D. Brabazon, "Nanoparticle production via laser ablation synthesis in solution method and printed electronic application - A brief review," *Results in Engineering*, vol. 16, p. 100646, Dec. 2022.

[37] S. S. Hallan, M. Sguizzato, E. Esposito, and R. Cortesi, "Challenges in the Physical Characterization of Lipid Nanoparticles," *Pharmaceutics*, vol. 13, no. 4, p. 549, Apr. 2021.

[38] V. R. Samuel and K. J. Rao, "A rapid colorimetric dual sensor for the detection of mercury and lead ions in water using cysteine-capped silver nanoparticles," *Chemical Physics Impact*, vol. 6, p. 100161, Jun. 2023.

[39] X. Zeng, W. Jiang, G. I. N. Waterhouse, X. Jiang, Z. Zhang, and L. Yu, "Stable Pb (II) ion-selective electrodes with a low detection limit using silver nanoparticles/polyaniline as the solid contact," *Microchim Acta*, vol. 188, no. 11, p. 393, Oct. 2021.

[40] Z. A. Tagar *et al.*, "Selective, simple and economical lead sensor based on ibuprofen derived silver nanoparticles," *Sensors and Actuators B: Chemical*, vol. 157, no. 2, pp. 430–437, Oct. 2011.

[41] Alankar Shrivastava and Vipin B. Gupta, "Methods for the determination of limit of detection and limit of quantitation of the analytical methods," vol. 2, no. 1, 2011.

[42] N. M. Razali, H. Mohamed, N. Abdullah, N. Safee, M. F. Omar, and S. Ambran, "Etched fiber Bragg grating sensor for lead ion detection," in *7th Brunei International Conference on Engineering and Technology 2018 (BICET 2018)*, Nov. 2018, pp. 1–4.

[43] T. Zhu, M. Loyez, K. Chah, and C. Caucheteur, "Gold-coated tilted fiber Bragg gratings for lead ion sensing," *Opt. Express, OE*, vol. 31, no. 20, pp. 32478–32487, Sep. 2023.

[44] C. Liu *et al.*, "Black phosphorus integrated tilted fiber grating for ultrasensitive heavy metal sensing," *Sensors and Actuators B: Chemical*, vol. 257, pp. 1093–1098, Mar. 2018.

[45] V. Kumar N, K. Bs, and S. Asokan, "Selective detection of lead in water using etched fiber Bragg grating sensor," *Sensors and Actuators B: Chemical*, vol. 354, p. 131208, Mar. 2022.

[46] N. Hidayat *et al.*, "Sensitivity enhancement of gold nanospheres assisted CO2 laser tapered optical fiber for refractive index sensor," *Optical Fiber Technology*, vol. 77, p. 103275, May 2023.

[47] T. K. Kori, A. Kori, A. Kori, and S. Nandi, "A Study on Fiber Bragg Gratings and Its Recent Applications," 2020, pp. 880–889.